

DOI: 10.1002/adma.200800030

## Tailoring Microporosity in Covalent Organic Frameworks\*\*

By R. William Tilford, Sam J. Mugavero III, Perry J. Pellechia, and John J. Lavigne\*

Microporous materials are proving to be invaluable tools, e.g., in the field of chemical separation,<sup>[1]</sup> catalysis,<sup>[2]</sup> and gas storage.<sup>[3]</sup> Function and utility of crystalline networks are often enhanced over those of more amorphous materials, which is largely due to the fact that they have well defined pore structures with a monodisperse size distribution, stable pores, and tunable metrics.<sup>[4]</sup> Previously, we,<sup>[5]</sup> as well as others,<sup>[6]</sup> reported the synthesis of covalently linked, highly crystalline covalent organic framework materials (COFs) based on boronate ester formation. Networks which are assembled via strong covalent bonds display improved stability over many coordinatively linked materials,<sup>[5,6,7]</sup> and exhibit enhanced pore stability once evacuated. It is therefore advantageous to develop methods to readily tailor the pore diameter and environment in covalently assembled structures, while maintaining structural homogeneity and pore size uniformity. Such a design diversifies and multiplies the number of applications in which this new class of microporous materials might find utility.

One approach to alter their framework structure exploits geometrically diverse starting materials.<sup>[6]</sup> However, while variation of the core monomer structure results in COFs with different pore sizes, observed structural changes are often inconsistent because changes in the fundamental geometry of the framework make a direct comparisons difficult. We therefore hypothesized that our facile synthetic approach would be applicable to the synthesis of networks which incorporate hydrophobic and sterically bulky groups (alkyl groups, i.e., methyl, ethyl, and propyl) in their pores while maintaining the same basic framework structure. Furthermore, we reasoned that we could use these substituents to tailor the pore size and therefore the adsorption properties of resulting COFs. To this end, we have developed the first modular assembly route which generates alkyl-functionalized, microporous COFs with pore diameters ranging from 1 to 2 nm. This straightforward approach, based on a catalyst free, facile dehydration technique at low temperature and ambient

pressure, allows us to tailor pore dimension and environment by condensing dialkyl-substituted bis-diols with triboric acids. A variety of COFs is generated in excellent yields by simple modification of the building blocks used in the synthesis. By employing this simple plug-n-play procedure, COFs containing pores of varying size that are lined with hydrophobic alkyl chains are readily synthesized. The gas adsorption properties of the resulting materials show that the incorporation of basic alkyl derivatives greatly influences the host capabilities of COFs.

Most previously reported methods for the formation of crystalline, porous materials utilize the self-assembly of monomeric units through non-covalent interactions to construct extended structures that possess a high degree of order.<sup>[8]</sup> For example crystal engineering,<sup>[9]</sup> strives to assemble organic 'monomers' in a predictable manner based on building block geometry and an anticipated solid-state packing. One of the greatest challenges to this approach is maintaining the porosity once the pores are evacuated.<sup>[10]</sup> Alternatively, transition metal ions or clusters may be employed to link organic monomer units through non-covalent or dative interactions, which results in materials commonly referred to as metal-organic frameworks (MOFs),<sup>[11]</sup> or metal-organic coordination networks (MOCNs).<sup>[12]</sup> While this type of assembly process often forms highly crystalline and stable porous structures, the incorporation of heavy metal atoms results in dense networks, thereby reducing the mass percentage of guest molecules that can be adsorbed into these materials.

Alternatively, techniques for the generation of microporous materials that are based on the assembly of single organic molecules, resulting in lighter frameworks that are capable of storing guest molecules in high weight percentages, have since emerged. For example, polymers exhibiting an intrinsic microporosity (PIMs),<sup>[13]</sup> incorporate contorted monomers which force the linear chains to pack into an arrangement that cannot avoid leaving voids within the matrix. Other microporous organic polymer-based networks rely on hyper-cross-linked polymers to provide more stable, covalently linked materials.<sup>[14]</sup> Although these materials are amorphous, they exhibit an exceptional thermal stability and somewhat high surface areas.

More recently, highly ordered, porous, covalently linked organic frameworks (COFs) have been assembled based on the interaction between boronic acids and diols.<sup>[5,6]</sup> The underlying boronate ester formation, which is covalent yet reversible in nature, maintains all of the desired attributes of self-assembling materials including ease of synthesis and

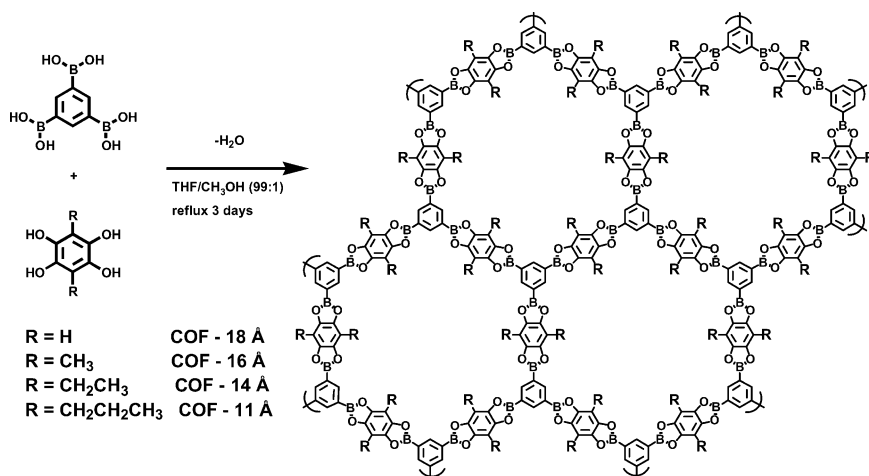
[\*] Prof. J. J. Lavigne, R. W. Tilford, S. J. Mugavero III, Dr. P. J. Pellechia  
Department of Chemistry and Biochemistry  
University of South Carolina  
631 Sumter St., Columbia, SC 29208 (USA)  
E-mail: lavigne@mail.chem.sc.edu

[\*\*] Financial support for this work was provided by the National Science Foundation (CHE-0415553, CHE-0718877). We also acknowledge Profs. Thomas Vogt and Hans Conrad zur Loye for helpful discussions. Supporting Information is available online from Wiley InterScience or from the author.

dynamic self-repair capability. The latter allows the monomers to assemble into a thermodynamically favored arrangement, which is often a highly crystalline form. At the same time, boronate linking produces stable covalently linked materials via a more facile route than conventional polymer synthesis.<sup>[7]</sup> These lightweight frameworks assemble into a highly ordered arrangement through a sequential dehydration process. The pores are thermally stable and persist when emptied of guest molecules.

Herein, we report on the synthesis, characterization, and gas adsorption properties of a series of alkyl (i.e., methyl, ethyl, and propyl) functionalized, microporous COFs formed via reaction of benzene-1,3,5-triboronic acid with dialkyl substituted derivatives of 1,2,4,5-tetrahydroxybenzene (Scheme 1). In order to obtain these alkylated COFs substituted bis-diol components were prepared as described in the supporting information. Reaction of the alkylated bis-diols with benzene-1,3,4-triboronic acid using the same reaction conditions that afforded the parent material COF-18Å,<sup>[5]</sup> subsequently yielded COF networks, as depicted in Scheme 1, indicates the pore diameter. COF-18Å (R = H), COF-16Å (R = methyl), and COF-14Å (R = ethyl) were isolated in yields of 95–99%, while COF-11Å (R = propyl) was obtained with 65% yield as they precipitated from solution. It is worth mentioning, that the formation of alkylated COFs requires a higher dilution than the generation of COF-18Å in order to avoid gelation of the reaction mixture. Therefore, twice the volume of tetrahydrofuran (THF) per mmol of boronic acid monomer was employed without increasing the volume of methanol.

Formation of the boronate ester linkages was verified using Fourier Transformed Infrared spectroscopy (FTIR) and solid state magic angle spinning (MAS) <sup>13</sup>C NMR. In the FTIR spectra, two intense peaks at 1300 and 1345 cm<sup>-1</sup> signify the presence of boronate containing species. A more distinct



**Scheme 1.** Synthesis of alkyl functionalized covalent organic frameworks (COFs) through condensation of benzene-1,3,5-triboronic acid and 2,6-disubstituted-1,2,4,5-tetrahydroxybenzene in THF and methanol.

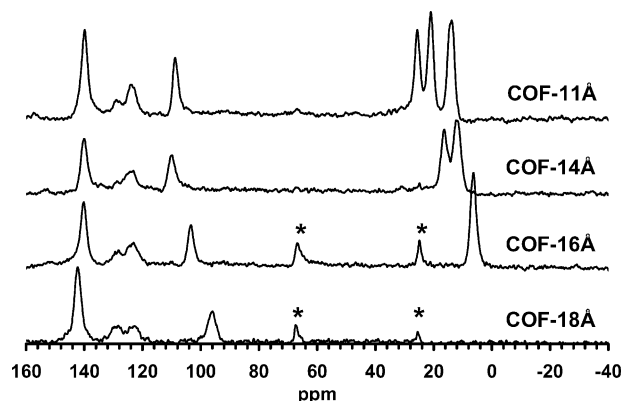


**Figure 1.** Solid state <sup>13</sup>C MAS NMR spectra of unsubstituted and alkyl modified COFs. The (\*) denotes resonances attributed to THF.

indicator for boronate ester formation is a sharp absorption at 640 cm<sup>-1</sup>, which was present in each of the COFs studied. The absence of any absorbances near 580 cm<sup>-1</sup> excludes the presence of boronate anhydride (boroxine) linkages.<sup>[15]</sup> The incorporation of alkyl chains into the substituted COFs was verified by the appearance of peaks between 2880 to 2970 cm<sup>-1</sup> in those samples.

In the <sup>13</sup>C MAS NMR spectra (Fig. 1) signals representing the aromatic resonances for the bis-diol and triboronic acid core structural components are observed between 90 and 150 ppm.<sup>[5,16]</sup> The presence of alkyl chains in the substituted COFs was verified by the appearance of resonances in the <sup>13</sup>C MAS NMR spectrum between 5–30 ppm. This analysis provides evidence that the framework assembly is not hindered by the presence of alkyl substituents on the bis-diol linker. Additionally, the networks were not evacuated for this analysis in order to demonstrate that the alkyl-functionalization alters the recognition properties of the pores. Signals that can be assigned to

solvent molecules (THF, 25 and 66 ppm) are present in the spectra of the two systems with larger pores, COF-18Å and COF-16Å, whereas no solvent is observed in the smaller pore materials COF-14Å and COF-11Å. The incorporation of alkyl chains into the matrix fills the pores and thereby reduces the diameter to such an extent that the THF molecules cannot fit in the pores of the later COFs. The fact that all COFs were dried under reduced pressure (0.5 mm Hg) at ambient temperature for 24 hours prior to NMR analysis indicates that the solvent is stored effectively within the larger pores. This illustrates that the introduction of hydrocarbon chains can alter the recognition and inclusion capabilities of COFs, thereby facilitating differentiation and size/guest selectivity dependent on the size of the alkyl substituent.

The thermal stability of alkylated COFs was monitored using thermogravimetric analysis (TGA).<sup>[17]</sup> All three alkylated COFs exhibited almost identical decomposition behavior to that of the parent network COF-18Å (see Supporting Information). Under anaerobic conditions, all networks began to break down just above 500 °C, and when heated in the presence of oxygen, degradation commences at approximately 300 °C. The incorporation of the side-chains does not alter the decomposition pattern, suggesting that the alkyl substituents are not thermally cleaved prior to network decomposition. Furthermore, upon heating the substituted COFs to 400 °C under high vacuum (<0.001 mm Hg) and maintaining this temperature for up to 24 h the appended alkyl chains are not cleaved from the framework as shown by FTIR analysis. This provides additional evidence for the thermal stability of the novel materials even at stringent conditions.

The conformational order and crystallinity of alkyl substituted COFs was confirmed using solid state <sup>11</sup>B NMR as well as powder X-ray diffraction (PXRD). <sup>11</sup>B NMR analysis confirmed the presence of tricoordinate, trigonal planar boron centers as indicated by the presence of a single peak between 26–28 ppm in the spectra of all alkyl substituted COFs.<sup>[18]</sup> Additionally, alkyl substituted COFs exhibited diffraction patterns similar to that observed for the parent material COF-18Å (Fig. 2). It is therefore reasoned that the novel COFs form ordered hexagonal networks of layered sheets which is similar to the structure assigned to COF-18Å.<sup>[5]</sup> The sheets assemble in a manner where atoms in adjacent layers lie directly on top of each other, giving rise to a hexagonal array of 1D pores. Given the geometric constraints within the system, it is further predicted that the alkyl substituents point towards the centre of the pores, thereby modifying pore size and environment. Like COF-18Å, COF-16Å is believed to be produced as a single phase material,<sup>[5]</sup> but given the broad signals in the PXRD patterns of COF-14Å and COF-11Å, it is difficult to confidently comment on the phase purity of these two COFs, although experiments described hereafter do support the formation of microporous networks.

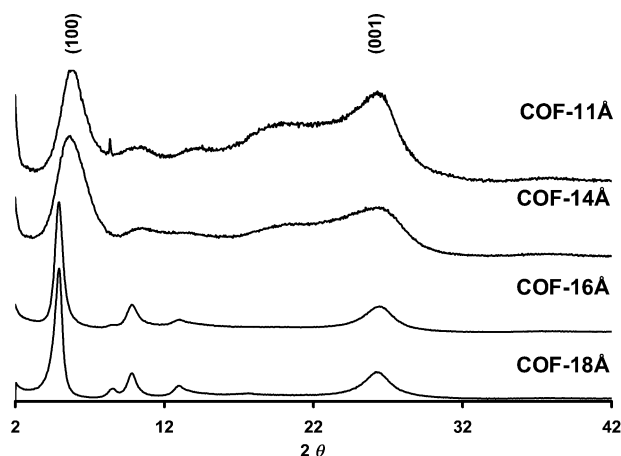


**Figure 2.** Powder X-ray diffraction (PXRD) patterns of alkylated COFs and their parent COF-18Å.

Specifically, COF-16Å produced a diffraction pattern almost identical to that of COF-18Å. COF-14Å and COF-11Å produced similar patterns with an overall broadening of peaks, particularly those at longer values of  $2\theta$ . This observation is consistent with the presence of amorphous units (i.e., flexible alkyl substituents) that freely rotate within the pores. Furthermore, the relative intensity of the (001) peak with respect to the (100) peak increased with increasing alkyl chain length. This change in peak intensities is caused by an increased number of atoms in the crystal planes along the *c*-axis upon addition of the alkyl groups, which results in greater diffraction from the added substituents. Additionally, the (100) peaks for COF-14Å and COF-11Å display asymmetric broadening towards smaller degrees  $2\theta$ . This trend results from the diffraction of carbon atoms attached to the pore walls which lie closer to each other than the atoms that constitute the framework.

Nitrogen gas adsorption of alkylated COFs resulted invariably in Type I isotherms (Fig. 3) which indicated that microporous networks were formed. Yet, they were clearly distinct from that of the parent material COF-18Å (measurements were taken at 77 K and  $P_0 = 760$  mm Hg, see Experimental for details). It was hypothesized that as the alkyl substituents become longer, the increased bulk would fill the pore thereby reducing the size and surface area of the pores. Additionally, the alkyl groups were also expected to create “pore corner cavities”, which block the access for nitrogen to the corners of the pores, hence reducing the surface area that is available for gas adsorption. As shown in Table 1, observed results are consistent with these hypotheses given that both, surface area (calculated using the BET method) and pore volume decrease as the length of alkyl substituent increases. Furthermore, COF-16Å and COF-14Å displayed almost identical adsorption isotherms until the point of saturation at  $P/P_0 = 1$ , with the methyl substituted COF showing a higher saturation point. It is noteworthy that, in replicate experiments, the ethyl substituted network exhibited a slightly larger surface area than the methyl functionalized COF. While both

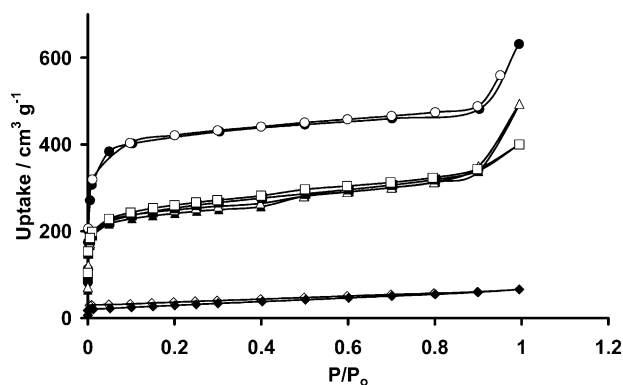


**Figure 3.** Nitrogen gas adsorption isotherms of substituted [COF-16Å (▲/△), COF-14Å (■/□), COF-11Å (◆/◇)] and unsubstituted [COF-18Å (●/○)] COFs. Black symbols correspond to adsorption; white symbols correspond to desorption. Measurements were taken at 77 K and  $P_0 = 760$  mm Hg.

**Table 1.** Gas Adsorption Data.

COF	Surface area [m <sup>2</sup> ·g <sup>-1</sup> ] [a]	Pore volume [cm <sup>3</sup> ·g <sup>-1</sup> ] [b]	N <sub>2</sub> uptake [wt%] [c]	N <sub>2</sub> uptake [mol N <sub>2</sub> /mol COF]	H <sub>2</sub> uptake [wt%] [d]	H <sub>2</sub> uptake [mol H <sub>2</sub> /mol COF]
COF-18 Å	1263	0.69	53.7	12.1	1.55	4.84
COF-16 Å	753	0.39	31.3	7.98	1.40	4.95
COF-14 Å	805	0.41	33.3	9.49	1.23	4.86
COF-11 Å	105	0.052	4.21	1.33	1.22	5.33

[a] Surface areas were calculated using N<sub>2</sub> gas adsorption isotherm data. [b] Pore volumes were calculated using N<sub>2</sub> gas adsorption data at  $P/P_0 = 0.30$ . [c] Uptake of N<sub>2</sub> by weight percent and mole fraction was calculated using data points at  $P/P_0 = 0.30$ . [d] Uptake of H<sub>2</sub> by weight percent and mole fraction was calculated using data points at  $P/P_0 = 1$ .

groups fill the pores and effectively block the access to pore corner cavities, the ethyl groups can rotate providing a larger surface for the nitrogen to adsorb onto, whereas the methyl groups do not provide as large a surface. Although COF-11Å still displayed an adsorption isotherm that is representative of microporous materials, its gas uptake was greatly diminished. Unlike the other three COFs, this network shows no sharp increase at the point of saturation, which suggests that the pores are saturated with nitrogen gas prior to its condensation at  $P/P_0 = 1$ .

We then reasoned that smaller gas molecules could possibly evade the alkyl groups that restrict access to the pore corner cavities, allowing us to gain insight into the availability of this region for guest adsorption. Therefore, we choose to analyze the gas adsorption properties of all COFs with hydrogen (measurements were taken at 77 K and  $P_0 = 760$  mm Hg) to further examine the nature of these micropores. In using this analysis method surfaces that are inaccessible for larger nitrogen molecules can be accessed. Hydrogen gas adsorption isotherms (Fig. 4) revealed a very much different uptake pattern for hydrogen compared to nitrogen at the same temperature, in that the isotherms of different COFs are quite similar to one another. COF-18Å showed the highest uptake of hydrogen with 1.5 wt%, whilst COF-11Å demonstrated an uptake of hydrogen exceeding 1.2 wt%. For comparison, while

hydrogen absorption was only attenuated by 20% between COF-18Å and COF-11Å, nitrogen uptake was diminished nearly tenfold. Given that hydrogen weighs less than nitrogen and the inclusion of alkyl substituents adds mass to the pores without altering the fundamental network structure, it is beneficial to compare the amount of gas adsorbed per pore (Table 1). Nitrogen adsorption per pore follows a trend similar to that observed for the calculated surface area, i.e., it decreases nearly an order of magnitude with incorporation of longer alkyl functionalities. However, the amount of hydrogen that can be stored per pore actually increased with increasing bulkiness of the alkyl group. Most likely, this does not only result from the ability of the smaller gas to access pore corner cavities, but also to adsorb to the incorporated alkyl groups as well, thereby increasing the amount of gas that can be stored per pore as longer alkyl substituents are added.

In summary, we showed for the first time that alkyl groups can be incorporated within the pores of covalent organic frameworks. This facile modification provides a simple way of tailoring the microporosity of the resultant frameworks. Added substituents minimally impacted on the synthesis, while greatly altering the host–guest properties of the resulting materials. Modification of the pore interior with increasingly larger alkyl groups causes a decline in nitrogen uptake but an increase in the molar amount of hydrogen adsorbed into the network. This work provides a model for the systematic study of the functionalization of microporous COFs. Future efforts are focused on generating more diversely functionalized materials.

## Experimental

**Materials:** 2,2,6,6-Tetramethylbenzo[1,2-*d*;4,5-*d'*]bis[1,3]dioxole (**1**) was obtained according to a literature procedure [19]. Benzene-1,3,5-triboronic acid and COF-18Å were synthesized as described previously [5]. All reagents were purchased from Acros and used without further purification, with the exception of *n*-butyl lithium which was purchased from Aldrich. All solvents used were obtained from solvent purification systems from Innovative Technologies.

**Instrumentation:** Solution <sup>1</sup>H and <sup>13</sup>C NMR spectra were collected on a Varian Mercury/VX 300 MHz spectrometer. Solid state <sup>11</sup>B and <sup>13</sup>C NMR spectra were collected on a Varian Inova 500 MHz spectrometer with a Doty 4 mm XC-MAS probe. FTIR spectra were collected on a Thermo Nicolet Nexus 470 FTIR ESP instrument with polished potassium chloride plates. Thermogravimetric analysis was carried out using a TA Instruments SDT 2960 DTA/TGA. Gas adsorption data were collected on a Quantachrome Autosorb-1

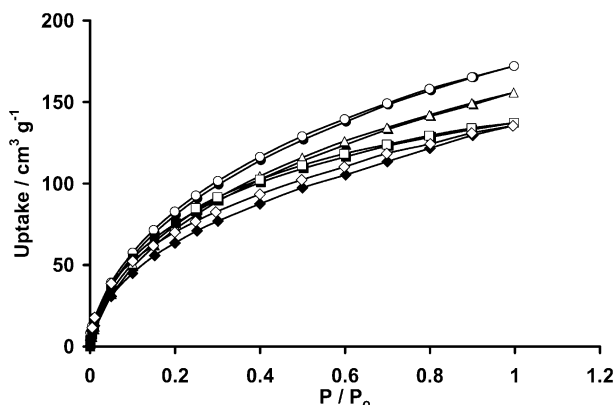


**Figure 4.** Hydrogen gas adsorption isotherms of substituted [COF-16Å (▲/△), COF-14Å (■/□), COF-11Å (◆/◇)] and unsubstituted [COF-18Å (●/○)] COFs. Black symbols correspond to adsorption; white symbols correspond to desorption. Measurements were taken at 77 K and  $P_0 = 760$  mm Hg.



automated analyzer. Powder X-ray diffraction patterns were collected on a Rigaku DMax 220 instrument using Cu K $\alpha$  radiation.

**General Procedure for the formation of COFs:** Benzene-1,3,5-triboronic acid (1 eq.) and the corresponding bis-diol (2 eq.) were dissolved in a mixture of THF (19.8 mL per mmol acid) and methanol (0.2 mL per mmol acid). The solution was refluxed under constant nitrogen flow for three days. The reaction mixture was cooled to room temperature and the fine suspension that was formed was collected by filtration. The solid was rinsed with THF (50 mL) and dried under vacuum (0.5 mm Hg) for 24 h.

**COF-16A:** Benzene-1,3,5-triboronic acid (215 mg, 0.81 mmol), bis-diol **3a** (303 mg, 1.78 mmol), THF (19.8 mL), methanol (0.2 mL); 276 mg obtained after rinsing with THF (50 mL) and vacuum drying; yield: 95%; Solid state MAS  $^{13}\text{C}$  NMR (125 MHz,  $\delta$ ): 6.0, 102.9, 122.3, 127.8, 139.8; Solid MAS  $^{11}\text{B}$  NMR (160.49 MHz,  $\text{BF}_3 \cdot \text{Et}_2\text{O}$  at 0 ppm as external reference and solid boric acid as second reference at 19.3 ppm,  $\delta$ ): 270; FTIR: 3500, 3250, 3050, 2950, 1610, 1340, 1300, 1190, 891, 704, 640  $\text{cm}^{-1}$ .

**COF-14A:** Benzene-1,3,5-triboronic acid (153 mg, 0.60 mmol), bis-diol **3b** (252 mg, 1.27 mmol), THF (19.8 mL), methanol (0.2 mL); 240 mg obtained after rinsing with THF (50 mL) and vacuum drying; yield: >99%; Solid state MAS  $^{13}\text{C}$  NMR (125 MHz,  $\delta$ ): 11.4, 15.9, 109.5, 122.8, 127.9, 139.6; Solid MAS  $^{11}\text{B}$  NMR (160.49 MHz,  $\text{BF}_3 \cdot \text{Et}_2\text{O}$  at 0 ppm as external reference and solid boric acid as second reference at 19.3 ppm,  $\delta$ ): 27.6; FTIR: 3470, 3250, 3060, 2970, 2940, 2880, 1600, 1340, 1300, 1120, 940, 723, 640  $\text{cm}^{-1}$ .

**COF-11A:** Benzene-1,3,5-triboronic acid (173 mg, 0.66 mmol), bis-diol **3c** (332 mg, 1.47 mmol), THF (19.8 mL), methanol (0.2 mL); 189 mg obtained after rinsing with THF (50 mL) and vacuum drying; yield: 65%; Solid state MAS  $^{13}\text{C}$  NMR (125 MHz,  $\delta$ ): 13.4, 20.9, 25.5, 108.6, 122.8, 127.9, 139.7; Solid MAS  $^{11}\text{B}$  NMR (160.49 MHz,  $\text{BF}_3 \cdot \text{Et}_2\text{O}$  at 0 ppm as external reference and solid boric acid as second reference at 19.3 ppm,  $\delta$ ): 27.3; FTIR: 3540, 3060, 2970, 2880, 1600, 1340, 1310, 1120, 964, 708, 660  $\text{cm}^{-1}$ .

**Thermogravimetric Analysis:** For the TGA plots shown 5–10 mg of sample was loaded onto an alumina dish and heated in the presence of oxygen. When samples were analyzed under a helium atmosphere, the major loss of mass occurred at approximately 500 °C. Prior to analysis, the samples were dried under mild vacuum (0.3–0.5 mm Hg) at ambient temperature for no more than 24 h.

**Powder X-ray Diffraction Analysis:** Samples were mounted on a deep well stainless steel slide. Data was collected from  $2\theta = 2^\circ$  to  $70^\circ$  in steps of  $0.02^\circ$  with a count time of 12 s per step. This analysis was carried out immediately after samples were filtered from the reaction mixture. After grinding the obtained solids using mortar and pestle, the fine powders were dried on a vacuum line (0.3–0.5 mm Hg) at ambient temperature for approximately 1–2 h. Samples were then analyzed.

**Gas Adsorption Analysis:** Gas adsorption data was collected using a liquid nitrogen bath for both nitrogen and hydrogen gas adsorption isotherms. Samples were prepared for analysis by suspending 25–50 mg of the COFs in 3 mL dry THF. After 24 h, the solvent was decanted and more THF was added to the vial. After additional 24 h, the solvent was decanted and the sample was dried on a vacuum line (0.3–0.5 mm Hg) at ambient temperature for 24 h. The dried powder was loaded into a 6 mm sample cell (small bulb) and degassed at 400 °C under high vacuum (<0.001 mm Hg) for 6–18 h.

Received: January 4, 2008

Revised: February 12, 2008

Published online: June 5, 2008

- [1] a) L. Alaerts, C. E. A. Kirschhock, M. Maes, M. van der Veen, V. Finsy, A. Depla, J. A. Martens, G. V. Baron, P. A. Jacobs, J. F. M. Denayer, D. E. De Vos, *Angew. Chem. Int. Ed.* **2007**, *46*, 4293; b) Q. M. Wang, D. Shen, M. Bulow, M. L. Lau, S. Deng, F. R. Fitch, N. O. Lemcoff, J. Semanscin, *Microporous Mater.* **2002**, *55*, 217.

- [2] a) S. Hasegawa, S. Horike, R. Matsuda, S. Furukawa, K. Mochizuki, Y. Kinoshita, S. Kitagawa, *J. Am. Chem. Soc.* **2007**, *129*, 2607; b) H. Ngo, W. Lin, *Top. Cat.* **2005**, *34*, 85.
- [3] a) J. L. C. Rowsell, O. M. Yaghi, *Angew. Chem. Int. Ed.* **2005**, *44*, 4670; b) R. Matsuda, R. Kitaura, S. Kitagawa, Y. Kubota, R. V. Belosludov, T. C. Kobayashi, H. Sakamoto, T. Chiba, M. Takata, Y. Kawazoe, Y. Mita, *Nature* **2005**, *436*, 238; c) P. M. Forster, J. Eckert, J. S. Chang, S.-E. Park, G. Férey, A. K. Cheetham, *J. Am. Chem. Soc.* **2003**, *125*, 1309; d) N. Rosi, J. Eckert, M. Eddaoudi, D. Vodak, J. Kim, M. O'Keeffe, O. M. Yaghi, *Science* **2003**, *300*, 1127; e) G. Férey, M. Latroche, C. Serre, F. Millange, A. Percheron-Guégan, *Chem. Commun.* **2003**, 2976; f) M. Eddaoudi, J. Kim, N. Rosi, D. Vodak, J. Wachter, M. O'Keeffe, O. M. Yaghi, *Science* **2002**, *295*, 469; g) J. L. C. Rowsell, A. R. Millward, K. S. Park, O. M. Yaghi, *J. Am. Chem. Soc.* **2004**, *126*, 5666.
- [4] O. M. Yaghi, M. O'Keeffe, N. W. Ockwig, H. K. Chae, M. Eddaoudi, J. Kim, *Nature* **2003**, *423*, 705.
- [5] R. W. Tilford, W. R. Gemmill, H. C. zur Loye, J. J. Lavigne, *Chem. Mater.* **2006**, *18*, 5296.
- [6] a) A. P. Cote, A. I. Benin, N. W. Ockwig, M. O'Keeffe, A. J. Matzger, O. M. Yaghi, *Science* **2005**, *310*, 1166; b) H. M. El-Kaderi, J. R. Hunt, J. L. Mendoza-Cortes, A. P. Cote, R. E. Taylor, M. O'Keeffe, O. M. Yaghi, *Science* **2007**, *316*, 268; c) A. P. Côté, H. M. El-Kaderi, H. Furukawa, J. R. Hunt, O. M. Yaghi, *J. Am. Chem. Soc.* **2007**, *129*, 12914.
- [7] W. Niu, C. O'Sullivan, B. M. Rambo, M. D. Smith, J. J. Lavigne, *Chem. Commun.* **2005**, 4342.
- [8] a) T. J. Barton, L. M. Bull, W. G. Klemperer, D. A. Loy, B. McEnaney, M. Misono, P. A. Monson, G. Pez, G. W. Scherer, J. C. Vartuli, O. M. Yaghi, *Chem. Mater.* **1999**, *11*, 2633; b) L. S. Shimizu, A. D. Hughes, M. D. Smith, M. J. Davis, B. P. Zhang, H.-C. zur Loye, K. D. Shimizu, *J. Am. Chem. Soc.* **2003**, *125*, 14972.
- [9] a) G. R. Desiraju, *Acc. Chem. Res.* **2002**, *35*, 565; b) L. Brammer, *Chem. Soc. Rev.* **2004**, *33*, 476; c) D. Braga, F. Grepioni, G. R. Desiraju, *Chem. Rev.* **1998**, *98*, 1375; d) B. Moulton, M. J. Zaworotko, *Chem. Rev.* **2001**, *101*, 1629.
- [10] a) S. Hasegawa, S. Horike, R. Matsuda, S. Furukawa, K. Mochizuki, Y. Kinoshita, S. Kitagawa, *J. Am. Chem. Soc.* **2007**, *129*, 2607; b) M. Eddaoudi, H. Li, O. M. Yaghi, *J. Am. Chem. Soc.* **2000**, *122*, 1391.
- [11] a) J. L. C. Rowsell, O. M. Yaghi, *Microporous Mater.* **2004**, *73*, 3; b) S. Kitagawa, R. Kitaura, S. Noro, *Angew. Chem. Int. Ed.* **2004**, *43*, 2334; c) C. Y. Su, A. M. Goforth, M. D. Smith, P. J. Pellechia, H. C. zur Loye, *J. Am. Chem. Soc.* **2004**, *126*, 3576; d) M. J. Rosseinsky, *Microporous Mater.* **2004**, *73*, 15; e) S. L. James, *Chem. Soc. Rev.* **2003**, *32*, 276; f) H. Eckert, M. Ward, special issue in *Chem. Mater.* **2001**, *13*, 3061; g) O. M. Yaghi, M. O'Keeffe, M. Kanatzidis, special issue in *J. Solid State Chem.* **2000**, *152*, 1; h) P. L. Hargman, D. Hargman, J. Zubietta, *Angew. Chem. Int. Ed.* **1999**, *38*, 2638.
- [12] a) O. R. Evans, W. Lin, *Acc. Chem. Res.* **2002**, *35*, 511; b) J. Moussa, K. Boubekeur, H. Amouri, *Eur. J. Inorg. Chem.* **2005**, 3808; c) J. Moussa, C. Guyard-Duhayon, K. Boubekeur, H. Amouri, S.-K. Yip, V. W. W. Yam, *Cryst. Growth Des.* **2007**, *7*, 962; d) J. Moussa, H. Amouri, *Angew. Chem. Int. Ed.* **2008**, *47*, 1372.
- [13] a) N. B. McKeown, P. M. Budd, *Chem. Soc. Rev.* **2006**, *35*, 675; b) H. J. Mackintosh, P. M. Budd, N. B. McKeown, *J. Mater. Chem.* **2008**, *18*, 573; c) B. S. Ghanem, K. J. Msayib, N. B. McKeown, K. D. M. Harris, Z. Pan, P. M. Budd, A. Butler, J. Selbie, D. Book, A. Walton, *Chem. Commun.* **2007**, 67; d) J. Weber, Q. Su, M. Antonietti, A. Thomas, *Macromol. Rapid Commun.* **2007**, *28*, 1871; e) P. M. Budd, A. Butler, J. Selbie, K. Mahmood, N. B. McKeown, B. Ghanem, K. Msayib, D. Book, A. Walton, *Phys. Chem. Chem. Phys.* **2007**, *9*, 1802; f) N. B. McKeown, P. M. Budd, D. Book, *Macromol. Rapid Commun.* **2007**, *28*, 995; g) N. B. McKeown, B. Ghanem, K. J. Msayib, P. M. Budd, C. E. Tattershall, K. Mahmood, S. Tan, D. Book, H. W. Langmi, A. Walton, *Angew. Chem. Int. Ed.* **2006**, *45*, 1804; h) P. M. Budd, N. B.

- McKeown, D. Fritsch, *J. Mater. Chem.* **2005**, *15*, 1977; i) P. M. Budd, E. S. Elabas, B. S. Ghanem, S. Makhseed, N. B. McKeown, K. J. Msayib, C. E. Tattershall, D. Wang, *Adv. Mater.* **2004**, *16*, 456.
- [14] a) C. D. Wood, B. Tan, A. Trewin, H. Niu, D. Bradshaw, M. J. Rosseinsky, Y. Z. Khimyak, N. L. Campbell, R. Kirk, E. Stoeckel, A. I. Cooper, *Chem. Mater.* **2007**, *19*, 2034; b) B. Pan, W. Du, W. Zhang, X. Zhang, Q. Zhang, B. Pan, L. Lv, Q. Zhang, J. Chen, *Environ. Sci. Technol.* **2007**, *41*, 5057; c) X. Zhang, S. Shen, L. Fan, *J. Mater. Sci.* **2007**, *42*, 7621; d) J. Y. Lee, C. D. Wood, D. Bradshaw, M. J. Rosseinsky, A. I. Cooper, *Chem. Commun.* **2006**, 2670; e) N. Fontanals, M. Galia, P. A. G. Cormack, R. M. Marce, D. C. Sherrington, F. Borrull, *J. Chromatogr. A* **2005**, *1075*, 51; f) L. M. Bronstein, G. Goerigk, M. Kostylev, M. Pink, I. A. Khotina, P. M. Valetsky, V. G. Matveeva, E. M. Sulman, M. G. Sulman, A. V. Bykov, N. V. Lakina, R. J. Spontak, *J. Phys. Chem. B* **2004**, *108*, 18234; g) M. P. Tsyurupa, V. A. Davankov, *React. Func. Polym.* **2002**, *53*, 193.
- [15] B. M. Rambo, J. J. Lavigne, *Chem. Mater.* **2007**, *19*, 3732.
- [16] Tetramethylsilane was used as external reference. Rapid quadrupolar relaxation associated with  $^{11}\text{B}$ - $^{13}\text{C}$  coupling results in a broadened signal for the *ipso*-carbon, and therefore this signal is often lost in the baseline noise and not observed in the  $^{13}\text{C}$  spectrum for phenylboronic acids: a) J. A. Pople, *Mol. Phys.* **1958**, *1*, 168; b) D. E. Axelson, A. J. Oliver, C. E. Holloway, *Org. Magn. Reson.* **1973**, *5*, 255; c) J. D. Odom, L. W. Hall, P. D. Ellis, *Org. Magn. Reson.* **1974**, *6*, 360.
- [17] It is noteworthy that the triboronic acid used in our COF syntheses has been studied as flame retardant material: a) A. B. Morgan, J. L. Jurs, J. M. Tour, *J. Appl. Polym. Sci.* **2000**, *76*, 1257.
- [18] a) In solution, tetrahedral boron exhibits a chemical shift of 0 ppm with respect to  $\text{BF}_3 \cdot \text{OEt}_2$  (defined as 0 ppm), while trigonal boron displays shifts closer to 30 ppm. Magic angle spinning solid state NMR analysis used boric acid as a solid reference at 19.3 ppm based on its solution analysis referenced to  $\text{BF}_3 \cdot \text{OEt}_2$  at 0 ppm; b) W. Niu, M. D. Smith, J. J. Lavigne, *Cryst. Growth Des.* **2006**, *6*, 1274; c) H. Noth, B. Wrackmeyer, *Nuclear Magnetic Resonance Spectroscopy of Boron Compounds in NMR-Basic Principles and Progress*, Vol. 14 (Eds: P. Diehl, E. Fluck, R. Kosfeld,) Springer, Berlin **1978**.
- [19] T. J. Reddy, T. Iwana, H. J. Halpern, V. H. Rawal, *J. Org. Chem.* **2002**, *67*, 4635.